



Article

Effects of High-Fat Diet on the Gut Microbiota of Renalase Gene Knockout Mice

Hui Fang¹, Kai Aoki^{2,3} , Katsuyuki Tokinoya^{3,4}, Masato Yonamine², Takehito Sugasawa², Yasushi Kawakami² and Kazuhiro Takekoshi^{2,*}

¹ Graduate School of Comprehensive Human Sciences, University of Tsukuba, Tsukuba 305-8577, Japan

² Faculty of Medicine, University of Tsukuba, Tsukuba 305-8577, Japan

³ Japan Society for the Promotion of Science, Kojimachi Business Center Building, Tokyo 102-0083, Japan

⁴ Department of Health Promotion Sciences, Graduate School of Human Health Sciences, Tokyo Metropolitan University, Hachioji-shi 192-0397, Japan

* Correspondence: k-takemd@md.tsukuba.ac.jp; Tel.: +81-029-853-3389

Abstract: Metabolic diseases caused by gene and unhealthy living habits are increasing, which seriously threaten the life of people worldwide. Moreover, the microbiome has been shown to play an active role in the prevention and treatment of metabolic diseases. However, reliable evidence on renalase gene (Rnls), as a common gene related to metabolic diseases, is still lacking with regard to the influence on the microbiome. Hence, we investigated the effect of a normal diet (ND) and a high-fat diet (HFD) on the gut microbiota of Rnls knockout (Rnls^{-/-}) and wild-type (Rnls^{+/+}) mice. At the end of the 8-week experiment, DNA samples were extracted from fresh feces, and the composition of microbiota was profiled. The species in Rnls^{+/+}-ND group were *Bifidobacterium pseudolongum* and *Lactobacillus reuteri*. Conversely, the species in Rnls^{-/-}-ND group belonged to the genera *Lactobacillus* and *Turicibacter*. The HFD changed the ratio of Firmicutes/Bacteroidetes; while the bacteria in the Rnls^{+/+}-HFD and Rnls^{-/-}-HFD groups were different. Overall, this study not only revealed the composition of microbiota in Rnls^{-/-} mice, but also indicated that Rnls and the bacteria related to Rnls may be new candidates in the prevention and diagnosis of metabolic diseases at an early stage.

Keywords: Rnls knockout; normal diet; high-fat diet; gut microbiota; Firmicutes/Bacteroidetes Tukey's post hoc test



Citation: Fang, H.; Aoki, K.; Tokinoya, K.; Yonamine, M.; Sugasawa, T.; Kawakami, Y.; Takekoshi, K. Effects of High-Fat Diet on the Gut Microbiota of Renalase Gene Knockout Mice. *Obesities* **2022**, *2*, 303–316. <https://doi.org/10.3390/obesities2030025>

Academic Editors: Yaohua Tian and Jixuan Ma

Received: 19 August 2022

Accepted: 6 September 2022

Published: 9 September 2022

Publisher's Note: MDPI stays neutral with regard to jurisdictional claims in published maps and institutional affiliations.



Copyright: © 2022 by the authors. Licensee MDPI, Basel, Switzerland. This article is an open access article distributed under the terms and conditions of the Creative Commons Attribution (CC BY) license (<https://creativecommons.org/licenses/by/4.0/>).

1. Introduction

The renalase gene (Rnls) was first discovered in 2005 as a flavoprotein oxidase [1]. It mainly regulates blood pressure and catecholamine metabolism. In recent years, Rnls has been suggested to suppress apoptosis, fibrosis, and inflammation [2,3], especially, the positive effect on gastrointestinal diseases [4]. A study carried out by our team showed that the absence of Rnls enhances oxidative stress, macrophage infiltration, and transforms growth factor- β expression in nonalcoholic steatohepatitis [5]. Moreover, another study identified that environmental oxidative stress changes Rnls expression in small intestinal crypts and overexpression of Rnls protects the Caco-2 cells against oxidative stress [6]. These results demonstrate the importance of Rnls in suppressing oxidative stress, apoptosis, and inflammation. It is well-known that progression of type 2 diabetes (T2D) is attributed to several factors, including inflammation and oxidative stress [7,8]. Together, it suggests that Rnls could have essential roles in modulating the progression of T2D. In addition, Rnls has been reported as a common polymorphism gene since it was discovered. For example, the rs2576178 polymorphism is common among patients with diabetes compared to those without; particularly rs2296545 and rs10887800 polymorphisms have been associated with hypertension and stroke among patients with type 2 diabetes (T2D) [9–12]. In other words, specific single-nucleotide polymorphisms of Rnls are highly related to increased risks of diabetes as well as complications. Nonetheless, the mechanism by which Rnls affects

diabetes and its complications is unknown, and considerable research is needed. T2D is most likely triggered by obesity and shows a significantly increasing trend [13]. The early detection of T2D aids in effective treatment and reduces morbidity. Hence, the potential mechanism involved in the effect of Rnls on obesity must be understood.

Intestinal microbiota plays an essential role in obesity and metabolic syndrome occurrence. Usually, the composition of the microbiome is considerably different in obese individuals compared to that in nonobese individuals; for example, bacteria of genera *Akkermansia*, *Faecalibacterium*, *Oscillibacter*, and *Alistipes* sharply decrease in obese individuals [14,15]. Similar results are also found by mouse models. Undoubtedly, HFD elevates the ratio of Firmicutes/Bacteroidetes in mice to increase the risk of obesity, aggravate intestinal dysfunction even systemic injury [16]. HFD decreases the abundance of some bacteria, such as *Akkermansia muciniphila*, which are positive reacting to weight loss, glucose, and lipid controlling [17]. Meanwhile, genotype is another factor to influence the composition of microbiota. According to intestinal microbiota genome-wide association studies, gene expression may affect intestinal microbial composition [18–21]. With in-depth development in research, association of a growing number of host genes with microbiota and diseases is confirmed. For example, the knockout of urate oxidase gene is related to the decreasing of *Akkermansia* and *Ruminococcus* and hyperuricemia. Moreover, apolipoprotein E, which relates to the development of insulin resistance also has been related to the influence on the composition of gut microbiota [22]. These results clearly indicate that the genotypic differences may have an overall enhancement in pathogenic behavior by controlling microbiota, thus reduces capabilities beneficial to health. Moreover, metabolism is influenced by metabolites from microbiota, including secondary bile acids, short-chain fatty acids, trimethylamine, farnesoid X receptor, activating G protein-coupled receptor, transmembrane G protein-coupled receptor5, phosphatidylinositol 3-kinase/Protein Kinase B (PI3K-AKT), and mitogen-activated protein kinase (MAPK), which improved inflammation and glucose/lipid metabolism [23–25]. A study revealed that *Akkermansia muciniphila* promotes the secretion of gut hormone glucagon-like peptide 1 for maintaining the homeostasis of glucose through the production of protein P9 and increases the thermogenesis of mice, leading to weight loss [17]. Moreover, according to intestinal microbiota genome-wide association studies, gene expression may affect intestinal microbial composition [18–21]. However, how Rnls affects the composition of gut microbiota and the underlying mechanism is still unclear, and substantial research in this area is warranted.

At present, no study compares the intestinal microbial composition of Rnls knockout mice under diet intervention; therefore, the effect of intestinal microbiota on metabolic disturbance remains unclear. Therefore, exploring the relationship between Rnls and microbiota composition is imperative. The present work focused on discovering differences in microbial abundances with or without Rnls and diet intervention.

2. Materials and Methods

2.1. Mice Management and Experimental Design

We obtained B6;129S1-Rnlstm1Gvd/J mice from the Jackson Laboratory. Mouse genomic DNA was subjected to polymerase chain reaction amplification according to the method described in a previous study to identify wild-type (Rnls^{+/+}) and Rnls knockout (Rnls^{-/-}) mice [5]. After obtaining the animals, they were housed in a room with 20–26 °C and 12-h/12-h light-dark cycle conditions. In total, 10 Rnls^{-/-} mice (male, 4-week-old) and 10 Rnls^{+/+} mice (male, 4-week-old) were acclimatized for 7 days and then grouped randomly. Mice were assigned different feeding routines for a total duration of 8 weeks (Figure 1). They were raised with a high-fat diet (HFD; Cat#D12492, 60 kcal% fat; Research Diets, New Brunswick, NJ, USA) or normal diet (ND; Cat#MF, Oriental Yeast, Itabashi, Tokyo, Japan), with free access to water. The fatty acids composition of HFD is shown in Table 1.

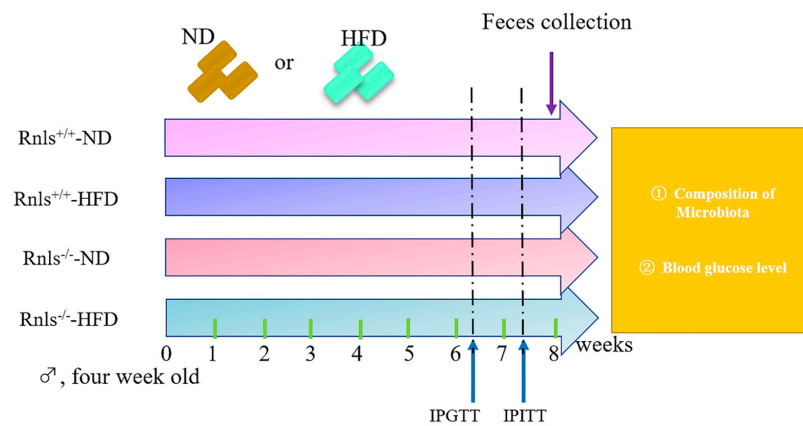


Figure 1. Experimental design. Mice were randomized into four groups: $Rnls^{-/-}$ -ND, $Rnls^{+/+}$ -ND, $Rnls^{-/-}$ -HFD, and $Rnls^{+/+}$ -HFD ($n = 5$ in each group). IPGTT and IPITT were conducted in the seventh and eighth weeks of the experiment, respectively. Fecal samples were collected weekly. ♂, male; $Rnls^{-/-}$ -ND, renalase gene knockout mice fed with normal diet; $Rnls^{+/+}$ -ND, wild-type mice fed with normal diet; $Rnls^{-/-}$ -HFD, renalase gene knockout mice fed with high-fat diet; $Rnls^{+/+}$ -HFD, wild-type mice fed with high-fat diet; IPITT, intraperitoneal insulin tolerance test; IPGTT, intraperitoneal glucose tolerance test.

Table 1. Typical composition of fats used by research diet (D12492).

Fatty Acids Name	Contents	Fatty Acids Name	Contents	Fatty Acids Name	Contents	Fatty Acids Name	Contents
C10, Capric	0.1	C16:1, Palmitoleic	3.4	C18:3, Linolenic	5.2	C20:4, Arachidonic	0.7
C12, Lauric	0.2	C17	0.9	C20, Arachidic	0.4	C22:5, Docospentaenoic	0.2
C14, Myristic	2.8	C18, Stearic	26.9	C20:1	1.5		
C15	0.2	C18:1, Oleic	86.6	C20:2	2.0		
C16, Palmitic	49.9	C18:2, Linoleic	73.1	C20:3	0.3		

Note: fatty acid profile was calculated based on assays of fats and oils performed in the 4th quarter of 2011. An example was given: D12492 was formatted by Lard (245 g) and soybean oil (25 g).

They were grouped as follows: $Rnls^{-/-}$ -HFD ($n = 5$) and $Rnls^{+/+}$ -HFD ($n = 5$) groups were fed HFD, whereas $Rnls^{-/-}$ -ND ($n = 5$) and $Rnls^{+/+}$ -ND ($n = 5$) groups were fed ND. A study reported placing mice on HFD (40–60% fat calories) for 8–12 weeks to induce obesity [26]. Therefore, HFD mice were raised with HFD (60% fat calories) for 8 weeks in our study. The ND mice were fed with ND for 8 weeks. In this study, we measured the body weight (BW) of mice every week. Additionally, we conducted an intraperitoneal insulin tolerance test (IPITT) and intraperitoneal glucose tolerance test (IPGTT) on the seventh and eighth weeks of the study, respectively. Feces were collected at the end of 8 weeks for gut microbiota analysis. Figure 1 presents the flowchart of the experimental design. Some details of the methods are described in the following sections. The Animal Subjects Committee, University of Tsukuba, Japan (approval number: 21-027), approved the study protocol.

2.2. Body Weight

BW of the mice was measured (to the nearest 0.1 g) every week until the end of 8 weeks. The weekly average BW of each group was calculated to record changes in BW during the experiment.

2.3. IPGTT and IPITT

The IPGTT was conducted on the seventh week of the experiment. In brief, 1–2 mm of the tail tip was cut off by using a pair of sharp scissors after subjecting the mice to overnight fasting. To avoid hemolysis and tissue fluid contamination, the first blood drop was eliminated before collecting samples to determine blood glucose (BG) levels. Approximately 3 μ L of blood was sampled to measure the baseline BG level (at time point 0) by using a glucometer (ACE-Quick, ACUU-CHEK, Roche, Basel, Switzerland).

Subsequently, the mice were administered glucose (20% D(+)-glucose, 2 mg/g BW) through intraperitoneal injection. Tail vein blood was sampled at 15-, 30-, 60-, and 120 min; the measurement method used was similar to that used at time point 0. After 1 week, IPITT was conducted. After 4 h of fasting, IPITT was conducted, and insulin was intraperitoneally injected into the mice (0.75 U/kg BW, Humulin-R; Lilly Research Labs, Indianapolis, IN, USA) to measure BG levels at time point 0 (pre-injection) and at time points 15-, 30-, 60-, and 120-min post-injection. Additionally, 20% glucose (D(+)-glucose solution was added to distilled water and injected into the hypoglycemic mice. We used GraphPad Prism 8.0.1 (GraphPad Software, Inc.) for calculating the area under the curve (AUC) for IPGTT. Data are presented as mean \pm standard deviation (SD).

2.4. Feces Collection

The feces of mice were collected at the end of the 8-week experiment. At first, 1.5-mL sterile tubes were labeled with Mouse ID (ID used on mouse shipment inventory sheet and/or in the colony); then, each mouse was individually placed into a clean cage without bedding to avoid the accumulation of mouse defecation in the cage; furthermore, plastic gloves were used to handle the mice. The fecal pellets were eliminated from the collection cage after the mice defecated 2–3 fecal pellets (~10 min). The fecal pellets were picked with sterile tweezers and placed into the 1.5-mL tubes marked with Mouse ID. The tubes with fecal samples were placed on ice until all samples were collected. The aforementioned steps were followed for all the housed mice. We changed gloves and collection cages while handling each sample to avoid contamination. The reuse of collection cages was permitted if used for the same mouse. The date and time of fecal collections were recorded. Once all samples were collected, the sample tubes were removed from the ice and placed in labeled baggies, which were preserved at -80°C until the extraction of feces DNA.

2.5. Feces DNA Extraction and 16S rRNA High Throughput Sequencing

Microbial genomic DNA from the fecal samples of mice ($n = 5$ per group) was extracted using the NucleoSpin DNA tool (U047A, Takara Bio, Tokyo, Japan) in line with specific protocols. The dual-indexed V3-V4-region primer (314F, 5'-TCGTCGGCAGCGTCAGATGTGTA TAAGAGACAGCTACGGGNGGCWGCAG-3', and 806R, 5'-GTCTCGTGGGCTCGGAGA TGTGTATAAGAGACAGGGATAACHVGGGTWTCTAAT-3'; Takara Bio, Japan) was used to amplify 16S ribosomal ribonucleic acid (rRNA) gene V3-V4 region by using barcodes. The PCR procedure was conducted using AMPure XP. PE300 sequencing was conducted using Illumina MiSeq. Quant iT dsDNA Assay Kit (Invitrogen, Thermo Fisher Scientific, San Jose, CA, USA) was used for evaluating library quality. The Illumina MiSeq platform was used for library sequencing followed by the generation of the 300-bp paired-end reads. Takara Bio, Japan, was responsible for the sequencing of the 16S rRNA gene. For generating taxon bins with a specific taxonomy, operational taxonomic units (OTUs) of identical taxonomic classification were pooled into one bin upon the threshold of 99% identity. Then, α - and β -diversity indexes were determined using quantitative insights into microbial ecology 2 (QIIME2) when analyzing microbial communities [27–29]. In addition, Shannon Diversity Index, Chao1, observed species OTUs, and Faith's phylogenetic diversity (Faithpd) were used for α -diversity calculations and for β -diversity distances, unweighted and weighted UniFrac were used to generate principal coordinate analysis (PCoA) plots [30]. R (<http://www.r-project.org/>, accessed on 19 August 2020) was used for generating the heatmap profile, whereas linear discriminant analysis (LDA) effect size (LEfSe) was used to elucidate differences in bacterial taxa. The cladogram was plotted using the LEfSe algorithm with the Huttenhower Galaxy web application (The Huttenhower Lab, Boston, MA, USA; <http://huttenhower.sph.harvard.edu/lefse/>, accessed on 19 August 2020).

2.6. Mice Euthanasia

After the experiment, the mice were euthanized through cervical dislocation under general anesthesia from isoflurane inhalation. The mice were anesthetized by placing them

in a closed bright evaporation glass container, and a large cotton ball with isoflurane was quickly put into this container and allowed to evaporate. We observed the mice's behavior closely during anesthesia. We observed that their respiratory frequency decreased and the depth increased, after which they were taken out for cervical dislocation. After euthanasia, mice were frozen in a $-20\text{ }^{\circ}\text{C}$ freezer in the animal carcass disposal room. All operations complied with animal ethics committee management standards.

2.7. Statistical Analysis

GraphPad Prism 8.0.1 (GraphPad Software. Inc., San Diego, CA, USA) was used for statistical analysis. Results are presented as mean \pm SD. This work used a two-way analysis of variance as well as Tukey's post hoc test for the analysis. The p value of <0.05 was considered for statistical significance.

3. Results

3.1. $Rnls^{-/-}$ Mice Fed with HFD for 8 Weeks Exhibited Impaired Glucose Tolerance

To evaluate the influence of $Rnls$ knockout and HFD on glucose homeostasis, we conducted IPGTT and IPITT. However, $Rnls^{-/-}$ and $Rnls^{+/+}$ mice fed with ND did not exhibit any difference (Figure 2A). Interestingly, BG levels were significantly high at 60 and 120 min in $Rnls^{-/-}$ mice compared with $Rnls^{+/+}$ mice under HFD (Figure 2A). Moreover, the glucose level of $Rnls^{-/-}$ mice under HFD increased quickly from 0 to 15 min (Figure 2A). For IPGTT, the AUC of $Rnls^{-/-}$ -HFD was the highest and differed from the other groups (Figure 2B). Subsequently, IPITT was conducted. Although HFD influenced the glucose level at 15 min after IPITT (Figure 2C), the AUC for IPITT did not significantly differ among the four groups (Figure 2D). Thus, no significant difference was observed in mice with or without $Rnls$ and HFD in terms of IPITT. Additionally, BW recorded weekly showed that the effect of HFD was the same in $Rnls^{+/+}$ and $Rnls^{-/-}$ mice (Figure 2E).

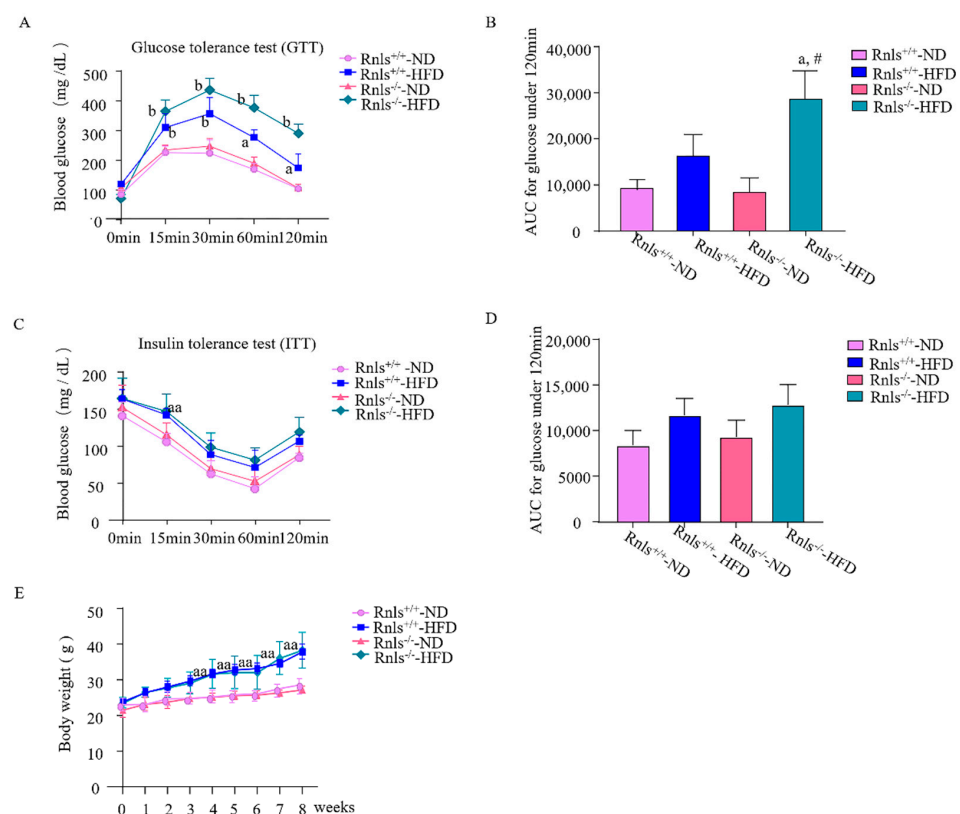


Figure 2. Phenotype of mice with or without $Rnls$ and food intervention. (A) IPGTT, (B) AUC for IPGTT, (C) IPITT, (D) AUC for IPITT, (E) body weight. Values are presented as mean \pm standard

derivation; $n = 5$ per group. Data are predicted through two-way ANOVA (Tukey's post hoc test) with repeated measures. a: $p < 0.05$, b: $p < 0.01$, indicating significant differences among diverse mouse groups compared with the $Rnls^{+/+}$ -ND group under the same timeline (time point or weeks). #: $p < 0.05$, indicating a significant difference compared with the $Rnls^{+/+}$ -HFD group. $Rnls^{-/-}$ -ND, renalase gene knockout mice fed with normal diet; $Rnls^{+/+}$ -ND, wild-type mice fed with normal diet; $Rnls^{-/-}$ -HFD, renalase gene knockout mice fed with high-fat diet; $Rnls^{+/+}$ -HFD, wild-type mice fed with high-fat diet; AUC, area under the curve; IPITT, intraperitoneal insulin tolerance test; IPGTT, intraperitoneal glucose tolerance test; ANOVA, analysis of variance.

3.2. Individual Taxa Richness and Evenness of Microbiota in $Rnls^{+/+}$ and $Rnls^{-/-}$ Mice

We used α diversity measures to identify within-individual taxa richness and evenness. The stable species rarefaction curve showed that sampling size (sequencing depth) data were large enough to reflect the majority of microbial diversity information in the sample and met the requirements for data analysis (Figure 3A). Shannon, Chao1, and Faith-pd indices indicated no significant difference in microbiota community diversity between the four groups (Figure 3B–D).

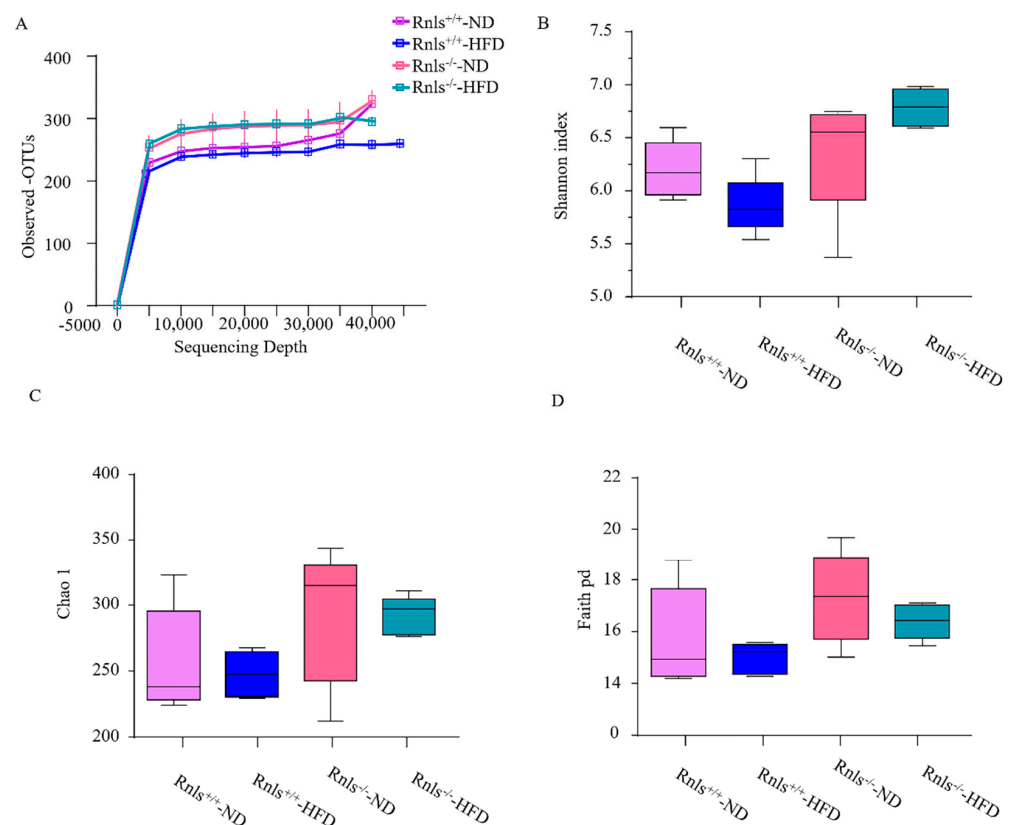


Figure 3. Rarefaction curves showing α -diversity indexes for bacterial communities based on 16S rRNA sequencing. (A–D) Intestinal microbial α -diversity in male $Rnls^{-/-}$ and $Rnls^{+/+}$ mice fed normal diet or high-fat diet. (A) Observed Species OTUs, (B) Shannon, (C) Chao1, and (D) Faith-pd. The Emperor α rarefaction was produced based on alpha_diversity.py script in QIIME 2. $Rnls^{-/-}$ -ND, renalase gene knockout mice fed with normal diet; $Rnls^{+/+}$ -ND, wild-type mice fed with normal diet; $Rnls^{-/-}$ -HFD, renalase gene knockout mice fed with high-fat diet; $Rnls^{+/+}$ -HFD, wild-type mice fed with high-fat diet; OTUs, operational taxonomic units, Faith-pd, Faith's phylogenetic diversity.

3.3. Microbial Distribution in $Rnls^{+/+}$ and $Rnls^{-/-}$ Mice

Thereafter, the total microbial diversities were compared across diverse groups based on weighted and unweighted UniFrac distance matrices. As expected, microbiota clustering was affected by $Rnls$ and diet. In Figure 4A, four distinct microbial clusters are exhibited, which indicate different microbiota compositions among the four groups. Weighted UniFrac

PCoA verified the identical clustering to some extent (Figure 4B), regardless of the limited graphical evidence.

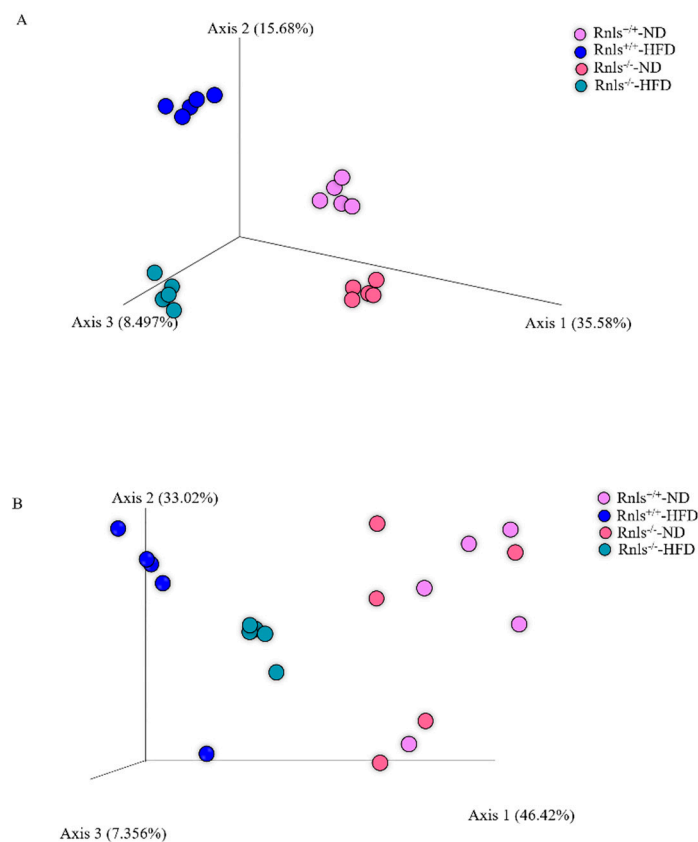


Figure 4. PCoA plot showing weighted and unweighted UniFrac distance matrices. **(A)** PCoA plots with unweighted UniFrac distance matrices illustrate distances between communities in all individual samples; different colors represent different groups. **(B)** PCoA plots with weighted UniFrac distance matrices illustrating distances between communities in all individual samples; different colors represent different groups. Generation of Emperor PCoA plots based on jackknifed_beta_diversity.py script in QIIME 2. Purple, $Rnls^{-/-}$ -ND, renalase gene knockout mice fed with normal diet; pink, $Rnls^{+/+}$ -ND, wild-type mice fed with normal diet; blue, $Rnls^{-/-}$ -HFD, renalase gene knockout mice fed with high-fat diet; cyan, $Rnls^{+/+}$ -HFD, wild-type mice fed with high-fat diet; PCoA, principal coordinate analysis.

3.4. Overall Compositions of Microbiota in $Rnls^{+/+}$ and $Rnls^{-/-}$ Mice

A total of 160 bacterial genera were observed among the four groups (Figure 5A), and each group maintained a unique microbiota. Venn diagrams revealed that $Rnls^{-/-}$ and $Rnls^{+/+}$ mice fed with ND had different microbiota (Figure 5A). To analyze the microbiota distribution in all the groups, the abundance of microbiota at the phylum level was first investigated. In mice fed with HFD, Firmicutes showed an increased abundance, whereas Bacteroidetes showed reduced abundance (Figure 5B). Notably, compared with the $Rnls^{+/+}$ -ND group, the $Rnls^{-/-}$ -ND group exhibited an increased Firmicutes abundance and decreased Bacteroidetes abundance (Figure 5B). Furthermore, the ratio of Firmicutes/Bacteroidetes was also calculated since it was related to obesity, and no difference was observed among the four groups (Figure 5B). Subsequently, microbiota distribution at the family level was analyzed. Similarly, the HFD groups had a decreased abundance of S24-7, *Lactobacillaceae*, and *Bifidobacteriaceae* while an increased abundance of *Ruminococcaceae*, *Clostridiales*, [Paraprevotellaceae], and *Desulfovibrionaceae* in comparison with the ND groups (Figure 5C). Statistically, the ratio of S24-7, *Lactobacillaceae*, *Ruminococcaceae*, and *Clostridiales* had a significant difference of HFD groups in comparison with ND

groups (Figure 5C). In addition, the ratio of S24-7 and *Desulfovibrionaceae* had a significant difference between $Rnls^{-/-}$ -HFD group and $Rnls^{+/+}$ -HFD group. Notably, the ratio of *Desulfovibrionaceae* only increased significantly in $Rnls^{+/+}$ -HFD group (Figure 5C).

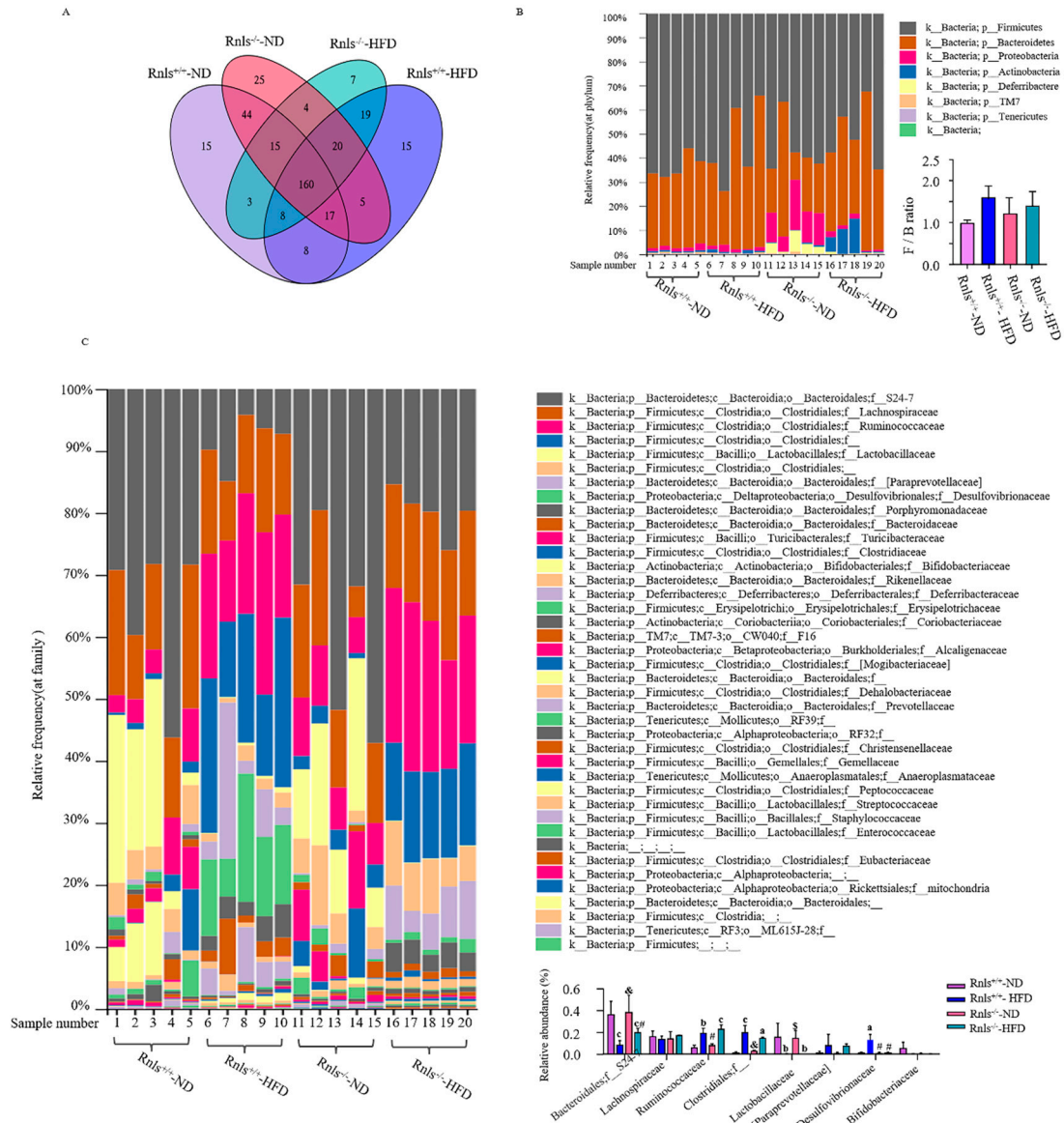


Figure 5. Relative microbial phylum and family abundances based on 16S ribosomal RNA gene sequencing. (A) Venn diagram showing OTUs among diverse groups. The 160 ‘core’ OTUs are shown. The mice of the $Rnls^{+/+}$ -ND, $Rnls^{-/-}$ -ND, $Rnls^{+/+}$ -HFD, and $Rnls^{-/-}$ -HFD groups presented 270, 290, 252, and 236 OTUs, respectively. The inside numbers represent the common OTUs among two or more samples and specific families. (B) Relative phylum abundances across $Rnls^{+/+}$ and $Rnls^{-/-}$ mice fed with HFD or ND. (C) Relative family abundances among $Rnls^{-/-}$ and $Rnls^{+/+}$ mice fed normal diet or high-fat diet. Data are predicted through two-way ANOVA (Tukey’s post hoc test) with repeated measures. a: $p < 0.05$, b: $p < 0.01$, c: $p < 0.001$ indicating significant differences among diverse mouse groups compared with the $Rnls^{+/+}$ -ND group. #: $p < 0.05$, \$: $p < 0.01$, &: $p < 0.001$ indicating a significant difference compared with the $Rnls^{+/+}$ -HFD group. $Rnls^{-/-}$ -ND, renalase gene knockout mice fed with normal diet; $Rnls^{+/+}$ -ND, wild-type mice fed with normal diet; $Rnls^{-/-}$ -HFD, renalase gene knockout mice fed with high-fat diet; $Rnls^{+/+}$ -HFD, wild-type mice fed with high-fat diet; F, Firmicutes; B, Bacteroidetes; OTU, operational taxonomic unit.

3.5. Significant Differences in Species Were Observed in the Microbiota of *Rnls*^{+/+} and *Rnls*^{-/-} Mice

To identify significant differences in species based on *Rnls*^{-/-} or diet, the fecal microbiota of the four groups were compared using LEfSe. The significant difference of species among the four groups at the genus level is presented in Figure 6. *Bifidobacterium pseudolongum* (*B. pseudolongum*) and *Lactobacillus reuteri* (*L. reuteri*) were the representative species in the *Rnls*^{+/+}-ND group, whereas the species belong to genera *Lactobacillus*, *Turicibacter*, and S24-7 were in the *Rnls*^{-/-}-ND group. Furthermore, the abundance of *Oscillospira*, *Parabacteroides*, *Anaerotruncus*, and *Anaerofustis* was high in the *Rnls*^{-/-}-HFD group, whereas the abundance of species belonging to genera *Bacteroides*, *Prevotella*, and *Mucispirillum* was high in the *Rnls*^{+/+}-HFD group.

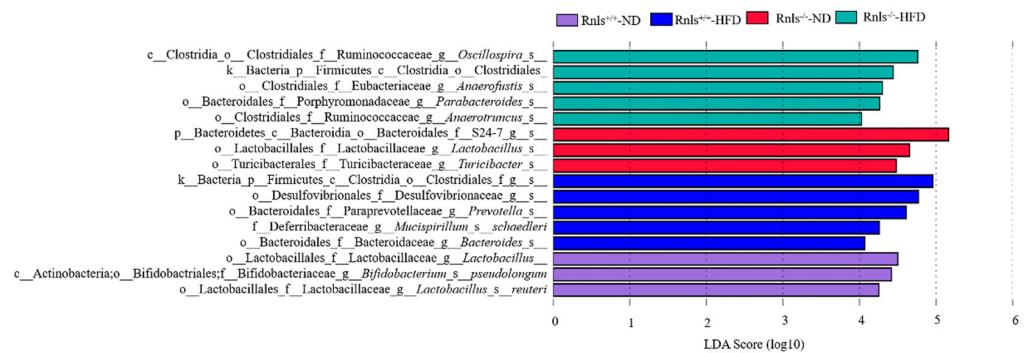


Figure 6. Significant difference in species in each group displayed using LDA scores. The distribution of LDA scores across species, with the X-axis representing LDA scores (Log10) and the Y-axis representing significantly different fecal bacterial species (LDA score > 4). *Rnls*^{-/-}-ND, renalase gene knockout mice fed with normal diet; *Rnls*^{+/+}-ND, wild-type mice fed with normal diet; *Rnls*^{-/-}-HFD, renalase gene knockout mice fed with high-fat diet; *Rnls*^{+/+}-HFD, wild-type mice fed with high-fat diet; LDA, linear discriminant analysis.

3.6. Dominant Patterns of Microbiota Composition in *Rnls*^{+/+} and *Rnls*^{-/-} Mice

To present the alteration in the overall composition of the dominant microbial community based on *Rnls* and HFD, a two-dimensional heatmap of the 20 most dominant orders was constructed (Figure 7). A hierarchical clustering based on the relative abundances of different orders could sufficiently differentiate between *Rnls*^{-/-} from *Rnls*^{+/+} mice. Bifidobacteriales exhibited high abundance in the *Rnls*^{+/+}-ND group compared with the other groups, whereas Lactobacillales exhibited high abundance in the *Rnls*^{+/+}-ND and *Rnls*^{-/-}-ND groups. Furthermore, the abundance of orders Coriobacteriales, Rickettsiales, and Erysipelotrichales was high in the *Rnls*^{+/+}-ND group, whereas the abundance of Turicibacterales, Bacteroidales, Burkholderiales, and Anaeroplasmatales was high in the *Rnls*^{-/-}-ND group. Clostridiales exhibited a high abundance in the *Rnls*^{+/+}-HFD and *Rnls*^{-/-}-HFD groups. The abundance of Desulfovibrionales, Deferribacterales, and Gemeliales was high in the *Rnls*^{+/+}-HFD group, whereas RF32 and RF39 had a high abundance in the *Rnls*^{-/-}-HFD group. Overall, our results illustrated the distinct patterns of gut bacterial composition in *Rnls*^{-/-} and *Rnls*^{+/+} mice under diet intervention.

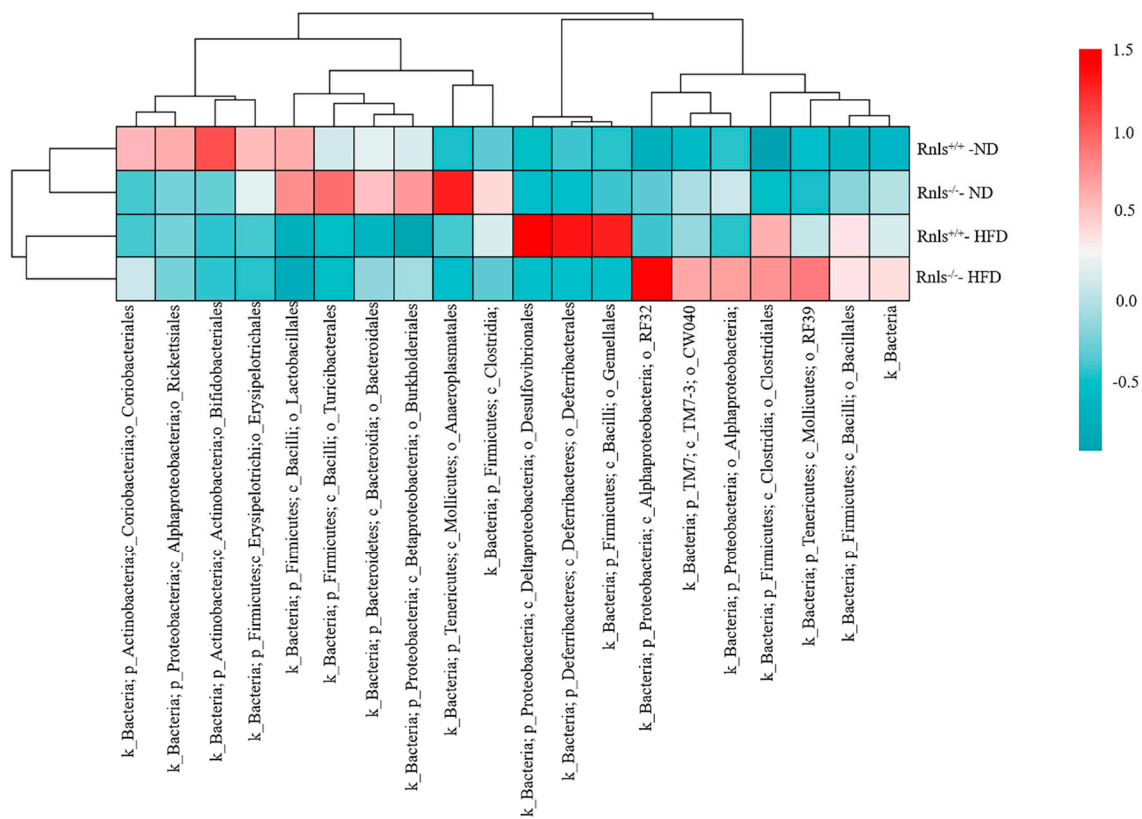


Figure 7. Heatmap of identified orders of dominant species among the four groups. The 20 species at the order level shared by all samples tested (core microbiome) are displayed. $Rnls^{-/-}$ -ND, renalase gene knockout mice fed with normal diet; $Rnls^{+/+}$ -ND, wild-type mice fed with normal diet; $Rnls^{-/-}$ -HFD, renalase gene knockout mice fed with high-fat diet; $Rnls^{+/+}$ -HFD, wild-type mice fed with a high-fat diet.

4. Discussion

In this work, HFD in $Rnls^{-/-}$ mice led to glucose tolerance impairment, but their BW was not significantly different from that of $Rnls^{+/+}$ mice (Figure 2A,B,E). This result proves that *Rnls* is associated with diabetes risk [11,31]. Diabetes is a metabolic disease characterized by hyperglycemia mainly because the liver is unable to effectively decrease the BG level through glycogen synthesis [32]. Glycogen synthesis is inseparable from high levels of AKT phosphorylation in the liver [33]. Notably, a study by our team showed that AKT phosphorylation in the liver decreased in $Rnls^{-/-}$ mice [5], which explains why the glucose level of mice in the $Rnls^{-/-}$ -HFD group during IPGTT decreased slowly compared to that in the other groups. In addition, extracellular *Rnls* exerts cell protection through the PI3K-AKT and MAPK pathways in different types of cells [34–36]. Obesity and diabetes are frequently accompanied by chronic inflammation, and *Rnls* knockout may reduce the innate ability against inflammation. Furthermore, it leads to impaired glycogen synthesis. According to various animal models [37,38], insulin resistance occurs before obesity until the age of 20 weeks. Our experimental period of 8 weeks is short, which may be the reason for the absence of distinct insulin resistance in Figure 2C,D. Additionally, the mice in the HFD group tended to develop insulin tolerance. The BG of mice in the $Rnls^{-/-}$ HFD group decreased slowly from 0 to 15 min after insulin injection compared to the ND group, which paves the way for metabolic disorder development.

In recent years, researchers have been focusing on microbiota as a vital aspect of metabolism. Genotype, growth, and diet habit affect microbiota distribution, which is further associated with obesity, diabetes, and its complications [21,23]. Owing to the close relationship between diabetes and microbiota, microbiota composition was well analyzed in our study. First, α diversity and β diversity were compared. We concluded that se-

quence depth is sufficient for all samples among the four groups and exhibited different clustering (Figures 3 and 4). Subsequently, microbiota composition was evaluated at the phylum level, order level, genus level, and so on. HFD remodeled the composition of the microbiota, such as S24-7, Lactobacillaceae, Ruminococcaceae, and Clostridiales (Figure 5). Moreover, the increased Firmicutes abundance and decreased Bacteroidetes abundance are coincident with dysbiosis microbiota and obesity caused by HFD [39,40]. Interestingly, $Rnls^{-/-}$ mice under ND also exhibited a high abundance of Firmicutes, which suggests that $Rnls$ knockout promotes the development of obesity or diabetes through changes in the proportions of Firmicutes and Bacteroidetes. For identifying significantly different species across groups, the LDA score was used in our study (Figure 6). *L. reuteri* and *B. pseudolongum* were considerably different in the $Rnls^{+/+}$ -ND group, and both have been described as probiotics in previous studies [41–43]. S24-7 and *Lactobacillus* were considerably different in the $Rnls^{-/-}$ -ND group, and both have been reported by decreasing the risk of obesity [44]. Moreover, we found that some bacteria are associated with T2D and obesity in the $Rnls^{+/+}$ -HFD, $Rnls^{-/-}$ -HFD and $Rnls^{-/-}$ -ND groups (Figure 6), such as *Prevotella*, *Bacteroides*, *Desulfovibrionaceae*, *Anaerotruncus*, and *Turicibacter* [14,45]. Increased abundance of *Anaerotruncus* and *Desulfovibrionaceae* were corroborated in human hypercholesterolemia patients [46]. Due to the increased abundance of these harmful bacteria, even though *Oscillospira* and *Parabacteroides* existed in $Rnls^{-/-}$ -HFD group, and they are beneficial to glucose metabolic and lipid metabolic pathways [47,48], they still did not exert a similar function as *L. reuteri* and *B. pseudolongum* of the $Rnls^{+/+}$ -ND group. Our results are consistent with previous studies, although genetic inheritance affects the establishment and configuration of microbiota, differences exist among bacterial populations, whereas some bacterial populations have the same function [15,49]. Our results suggest that $Rnls$ knockout possibly affects the composition of microbiota and abundance of some bacteria. Additionally, to evaluate the dominant species among the four groups, the top 20 orders of species were displayed using a heatmap. The bacteria of orders Lactobacillales and Bifidobacteriales were dominant in the $Rnls^{+/+}$ -ND group, whereas bacteria of the orders Lactobacillales and Anaeroplasmatales were dominant in the $Rnls^{-/-}$ -ND group. Clostridiales were the dominant bacteria in the HFD group (Figure 7). Overall, $Rnls$ and the bacteria related to $Rnls$ may be new candidates in the prevention and diagnosis of diabetes at an early stage, as previous studies have suggested [9,50].

Moreover, mouse models are important tools for studying the pathogenesis and treatment of metabolic diseases, because they share a distinct genetic similarity to humans and are also economically efficient for scientific study. In our study, we demonstrated that the composition of microbiota was closely related to $Rnls$ knockout. These results confirm the advantages of mice as an experimental model again. Over the years, many mouse models have been developed and have provided valuable insights to the pathogenesis of metabolic diseases with no doubt. Of course, our study is no exception. The potential of $Rnls$ as predictors of metabolic diseases was provided. However, since almost all mouse models can only mimic specific features, to understand well the occurrence and progression of human diseases, a lot of work still need to be done in the future.

5. Conclusions

$Rnls$ knockout leads to glucose tolerance impairment and intestinal microbial disruption in mice. Furthermore, $Rnls$ knockout increased the abundance of bacteria belonging to the Firmicutes phylum and decreased the abundance of those belonging to Bacteroidetes. Moreover, $Rnls$ may regulate the abundance of genera *Lactobacillus* and *Turicibacter* under ND, and *Oscillospira*, *Parabacteroides*, and *Anaerotruncus* under HFD. $Rnls^{-/-}$ mice exhibited glucose intolerance compared to $Rnls^{+/+}$ mice under HFD. Overall, $Rnls$ knockout may accelerate dysbiosis of microbiota, increasing the risk of metabolic diseases.

Author Contributions: H.F. designed and performed this study. K.A. and M.Y. substantially contributed to writing the paper. Y.K., K.A., K.T. (Katsuyuki Tokinoya), T.S., and M.Y. contributed to performing the experiments and data analysis. K.T. (Kazuhiro Takekoshi) supervised the study, conducted the formal analysis, and acquired funding. All authors have read and agreed to the published version of the manuscript.

Funding: This work was supported by JST SPRING, grant number is JPMJSP2124.

Institutional Review Board Statement: The study was approved by the Animal Subjects Committee, University of Tsukuba, Japan (approval number: 21-027).

Data Availability Statement: Data are available upon request from k-takemd@md.tsukuba.ac.jp.

Acknowledgments: We are grateful to Seiko Ono and Takuro Nakano for their technical guidance during animal experiment.

Conflicts of Interest: The authors declare that they have no known competing financial interests or personal relationships that could have appeared to influence the work reported in this paper.

References

1. Xu, J.; Li, G.; Wang, P.; Velazquez, H.; Yao, X.; Li, Y.; Wu, Y.; Peixoto, A.; Crowley, S.; Desir, G.V. Renalase is a novel, soluble monoamine oxidase that regulates cardiac function and blood pressure. *J. Clin. Investig.* **2005**, *115*, 1275–1280. [[CrossRef](#)] [[PubMed](#)]
2. Wu, Y.; Wang, L.; Wang, X.; Wang, Y.; Zhang, Q.; Liu, W. Renalase contributes to protection against renal fibrosis via inhibiting oxidative stress in rats. *Int. Urol. Nephrol.* **2018**, *50*, 1347–1354. [[CrossRef](#)] [[PubMed](#)]
3. Li, X.; Xie, Z.; Lin, M.; Huang, R.; Liang, Z.; Huang, W.; Jiang, W. Renalase Protects the Cardiomyocytes of Sprague-Dawley Rats Against Ischemia and Reperfusion Injury by Reducing Myocardial Cell Necrosis and Apoptosis. *Kidney Blood Press. Res.* **2015**, *40*, 215–222. [[CrossRef](#)]
4. Pointer, T.; Gorelick, F.; Desir, G. Renalase: A Multi-Functional Signaling Molecule with Roles in Gastrointestinal Disease. *Cells* **2021**, *10*, 2006. [[CrossRef](#)]
5. Tokinoya, K.; Sekine, N.; Aoki, K.; Ono, S.; Kuji, T.; Sugasawa, T.; Yoshida, Y.; Takekoshi, K. Effects of renalase deficiency on liver fibrosis markers in a nonalcoholic steatohepatitis mouse model. *Mol. Med. Rep.* **2021**, *23*, 210. [[CrossRef](#)]
6. Aoki, K.; Yanazawa, K.; Tokinoya, K.; Sugasawa, T.; Suzuki, T.; Yoshida, Y.; Nakano, T.; Omi, N.; Kawakami, Y.; Takekoshi, K. Renalase is localized to the small intestine crypt and expressed upon the activation of NF- κ B p65 in mice model of fasting-induced oxidative stress. *Life Sci.* **2020**, *267*, 118904. [[CrossRef](#)]
7. Luc, K.; Schramm-Luc, A.; Guzik, T.J.; Mikolajczyk, T.P. Oxidative stress and inflammatory markers in prediabetes and diabetes. *J. Physiol. Pharmacol.* **2019**, *70*, 70. [[CrossRef](#)]
8. Vassalle, C.; Gaggini, M. Type 2 Diabetes and Oxidative Stress and Inflammation: Pathophysiological Mechanisms and Possible Therapeutic Options. *Antioxidants* **2022**, *11*, 953. [[CrossRef](#)]
9. Lafferty, R.A.; O'Harte, F.P.M.; Irwin, N.; Gault, V.A.; Flatt, P.R. Proglucagon-Derived Peptides as Therapeutics. *Front. Endocrinol.* **2021**, *12*, 689678. [[CrossRef](#)]
10. Teimoori, B.; Moradi-Shahrehabak, M.; Rezaei, M.; Mohammadpour-Gharehbagh, A.; Salimi, S. Renalase rs10887800 polymorphism is associated with severe pre-eclampsia in southeast Iranian women. *J. Cell. Biochem.* **2018**, *120*, 3277–3285. [[CrossRef](#)]
11. Buraczynska, M.; Gwiazda-Tyndel, K.; Drop, B.; Zaluska, W. Renalase gene Glu37Asp polymorphism affects susceptibility to diabetic retinopathy in type 2 diabetes mellitus. *Geol. Rundsch.* **2021**, *58*, 1595–1602. [[CrossRef](#)]
12. Zhang, F.; Liu, W.; Wu, Y.; Li, X.; Zhang, S.; Feng, Y.; Lu, R.; Sun, L. Association of renalase gene polymorphisms with the risk of hypertensive disorders of pregnancy in northeastern Han Chinese population. *Gynecol. Endocrinol.* **2020**, *36*, 986–990. [[CrossRef](#)]
13. Saeedi, P.; Petersohn, I.; Salpea, P.; Malanda, B.; Karuranga, S.; Unwin, N.; Colagiuri, S.; Guariguata, L.; Motala, A.A.; Ogurtsova, K.; et al. Global and regional diabetes prevalence estimates for 2019 and projections for 2030 and 2045: Results from the International Diabetes Federation Diabetes Atlas, 9th edition. *Diabetes Res. Clin. Pract.* **2019**, *157*, 107843. [[CrossRef](#)]
14. Thingholm, L.B.; Rühlemann, M.C.; Koch, M.; Fuqua, B.; Laucke, G.; Boehm, R.; Bang, C.; Franzosa, E.A.; Hübenenthal, M.; Rahnavard, G.; et al. Obese Individuals with and without Type 2 Diabetes Show Different Gut Microbial Functional Capacity and Composition. *Cell Host Microbe* **2019**, *26*, 252–264.e10. [[CrossRef](#)]
15. Turnbaugh, P.J.; Hamady, M.; Yatsunencko, T.; Cantarel, B.L.; Duncan, A.; Ley, R.E.; Sogin, M.L.; Jones, W.J.; Roe, B.A.; Affourtit, J.P.; et al. A core gut microbiome in obese and lean twins. *Nature* **2009**, *457*, 480–484. [[CrossRef](#)]
16. Yang, F.; Zhu, W.-J.; Edirisuriya, P.; Ai, Q.; Nie, K.; Ji, X.-M.; Li, Y.; Zhou, K. Beneficial effects of a combination of *Clostridium cochlearium* and *Lactobacillus acidophilus* on body weight gain, insulin sensitivity, and gut microbiota in high-fat diet-induced obese mice. *Nutrition* **2021**, *93*, 111439. [[CrossRef](#)]
17. Yoon, H.S.; Cho, C.H.; Yun, M.S.; Jang, S.J.; You, H.J.; Kim, J.-H.; Han, D.; Cha, K.H.; Moon, S.H.; Lee, K.; et al. Akkermansia muciniphila secretes a glucagon-like peptide-1-inducing protein that improves glucose homeostasis and ameliorates metabolic disease in mice. *Nat. Microbiol.* **2021**, *6*, 563–573. [[CrossRef](#)]

18. Davenport, E.R. Elucidating the role of the host genome in shaping microbiome composition. *Gut Microbes* **2016**, *7*, 178–184. [[CrossRef](#)]
19. Goodrich, J.K.; Davenport, E.R.; Clark, A.G.; Ley, R.E. The Relationship Between the Human Genome and Microbiome Comes into View. *Annu. Rev. Genet.* **2017**, *51*, 413–433. [[CrossRef](#)] [[PubMed](#)]
20. Liu, X.; Tong, X.; Zhu, J.; Tian, L.; Jie, Z.; Zou, Y.; Lin, X.; Liang, H.; Li, W.; Ju, Y.; et al. Metagenome-genome-wide association studies reveal human genetic impact on the oral microbiome. *Cell Discov.* **2021**, *7*, 117. [[CrossRef](#)] [[PubMed](#)]
21. Liu, X.; Tang, S.; Zhong, H.; Tong, X.; Jie, Z.; Ding, Q.; Wang, D.; Guo, R.; Xiao, L.; Xu, X.; et al. A genome-wide association study for gut metagenome in Chinese adults illuminates complex diseases. *Cell Discov.* **2021**, *7*, 9. [[CrossRef](#)] [[PubMed](#)]
22. Zajac, D.J.; Green, S.J.; Johnson, L.A.; Estus, S. APOE genetics influence murine gut microbiome. *Sci. Rep.* **2022**, *12*, 1906. [[CrossRef](#)] [[PubMed](#)]
23. Kumar, J.; Rani, K.; Datt, C. Molecular link between dietary fibre, gut microbiota and health. *Mol. Biol. Rep.* **2020**, *47*, 6229–6237. [[CrossRef](#)] [[PubMed](#)]
24. Wang, K.; Liao, M.; Zhou, N.; Bao, L.; Ma, K.; Zheng, Z.; Wang, Y.; Liu, C.; Wang, W.; Wang, J.; et al. Parabacteroides distasonis Alleviates Obesity and Metabolic Dysfunctions via Production of Succinate and Secondary Bile Acids. *Cell Rep.* **2019**, *26*, 222–235.e5. [[CrossRef](#)]
25. Schoeler, M.; Caesar, R. Dietary lipids, gut microbiota and lipid metabolism. *Rev. Endocr. Metab. Disord.* **2019**, *20*, 461–472. [[CrossRef](#)]
26. Nagy, C.; Einwallner, E. Study of In Vivo Glucose Metabolism in High-fat Diet-fed Mice Using Oral Glucose Tolerance Test (OGTT) and Insulin Tolerance Test (ITT). *J. Vis. Exp.* **2018**, *131*, e56672. [[CrossRef](#)]
27. Beck, D.; Foster, J. Machine Learning Techniques Accurately Classify Microbial Communities by Bacterial Vaginosis Characteristics. *PLoS ONE* **2014**, *9*, e87830. [[CrossRef](#)]
28. Yatsunenkov, T.; Rey, F.E.; Manary, M.J.; Trehan, I.; Dominguez-Bello, M.G.; Contreras, M.; Magris, M.; Hidalgo, G.; Baldassano, R.N.; Anokhin, A.P.; et al. Human gut microbiome viewed across age and geography. *Nature* **2012**, *486*, 222–227. [[CrossRef](#)]
29. Kaul, A.; Davidov, O.; Peddada, S.D. Structural zeros in high-dimensional data with applications to microbiome studies. *Biostatistics* **2017**, *18*, 422–433. [[CrossRef](#)] [[PubMed](#)]
30. Yu, D.; Yu, X.; Ye, A.; Xu, C.; Li, X.; Geng, W.; Zhu, L. Profiling of gut microbial dysbiosis in adults with myeloid leukemia. *FEBS Open Bio* **2021**, *11*, 2050–2059. [[CrossRef](#)]
31. Czubińska-Lada, J.; Gliwińska, A.; Badeński, A.; Szczepańska, M. Associations between renalase concentration and the occurrence of selected diseases. *Endokrynol. Polska* **2020**, *71*, 334–342. [[CrossRef](#)] [[PubMed](#)]
32. Cui, X.; Qian, D.-W.; Jiang, S.; Shang, E.-X.; Zhu, Z.-H.; Duan, J.-A. Scutellariae Radix and Coptidis Rhizoma Improve Glucose and Lipid Metabolism in T2DM Rats via Regulation of the Metabolic Profiling and MAPK/PI3K/Akt Signaling Pathway. *Int. J. Mol. Sci.* **2018**, *19*, 3634. [[CrossRef](#)] [[PubMed](#)]
33. Liu, T.-Y.; Shi, C.-X.; Gao, R.; Sun, H.-J.; Xiong, X.-Q.; Ding, L.; Chen, Q.; Li, Y.-H.; Wang, J.-J.; Kang, Y.-M.; et al. Irisin inhibits hepatic gluconeogenesis and increases glycogen synthesis via the PI3K/Akt pathway in type 2 diabetic mice and hepatocytes. *Clin. Sci.* **2015**, *129*, 839–850. [[CrossRef](#)] [[PubMed](#)]
34. Guo, X.; Hollander, L.; MacPherson, D.; Wang, L.; Velazquez, H.; Chang, J.; Safirstein, R.; Cha, C.; Gorelick, F.; Desir, G.V. Inhibition of renalase expression and signaling has antitumor activity in pancreatic cancer. *Sci. Rep.* **2016**, *6*, 22996. [[CrossRef](#)] [[PubMed](#)]
35. Wang, L.; Velazquez, H.; Moeckel, G.; Chang, J.; Ham, A.; Lee, H.T.; Safirstein, R.; Desir, G.V. Renalase Prevents AKI Independent of Amine Oxidase Activity. *J. Am. Soc. Nephrol.* **2014**, *25*, 1226–1235. [[CrossRef](#)]
36. Tokinoya, K.; Shiromoto, J.; Sugawara, T.; Yoshida, Y.; Aoki, K.; Nakagawa, Y.; Ohmori, H.; Takekoshi, K. Influence of acute exercise on renalase and its regulatory mechanism. *Life Sci.* **2018**, *210*, 235–242. [[CrossRef](#)]
37. Barnard, R.; Faria, D.J.; Menges, J.E.; Martin, D.A. Effects of a high-fat, sucrose diet on serum insulin and related atherosclerotic risk factors in rats. *Atherosclerosis* **1993**, *100*, 229–236. [[CrossRef](#)]
38. Barnard, R.J.; Roberts, C.K.; Varon, S.M.; Berger, J.J. Diet-induced insulin resistance precedes other aspects of the metabolic syndrome. *J. Appl. Physiol.* **1998**, *84*, 1311–1315. [[CrossRef](#)]
39. Zhao, L.; Zhang, Q.; Ma, W.; Tian, F.; Shen, H.; Zhou, M. A combination of quercetin and resveratrol reduces obesity in high-fat diet-fed rats by modulation of gut microbiota. *Food Funct.* **2017**, *8*, 4644–4656. [[CrossRef](#)]
40. Lu, L.; Tang, M.; Li, J.; Xie, Y.; Li, Y.; Xie, J.; Zhou, L.; Liu, Y.; Yu, X. Gut Microbiota and Serum Metabolic Signatures of High-Fat-Induced Bone Loss in Mice. *Front. Cell. Infect. Microbiol.* **2021**, *11*, 788576. [[CrossRef](#)]
41. Yang, B.; Zheng, F.; Stanton, C.; Ross, R.P.; Zhao, J.; Zhang, H.; Chen, W. *Lactobacillus reuteri* FYNL109L1 Attenuating Metabolic Syndrome in Mice via Gut Microbiota Modulation and Alleviating Inflammation. *Foods* **2021**, *10*, 2081. [[CrossRef](#)] [[PubMed](#)]
42. Zhang, C.; Fang, R.; Lu, X.; Zhang, Y.; Yang, M.; Su, Y.; Jiang, Y.; Man, C. *Lactobacillus reuteri* J1 prevents obesity by altering the gut microbiota and regulating bile acid metabolism in obese mice. *Food Funct.* **2022**, *13*, 6688–6701. [[CrossRef](#)] [[PubMed](#)]
43. Xiao, Y.; Zhao, J.; Zhang, H.; Zhai, Q.; Chen, W. Colonized Niche, Evolution and Function Signatures of *Bifidobacterium pseudolongum* within Bifidobacterial Genus. *Foods* **2021**, *10*, 2284. [[CrossRef](#)] [[PubMed](#)]
44. Lieber, A.D.; Beier, U.H.; Xiao, H.; Wilkins, B.J.; Jiao, J.; Li, X.S.; Schugar, R.C.; Strauch, C.M.; Wang, Z.; Brown, J.M.; et al. Loss of HDAC6 alters gut microbiota and worsens obesity. *FASEB J.* **2018**, *33*, 1098–1109. [[CrossRef](#)]

45. Yuan, G.; Tan, M.; Chen, X. Punicic acid ameliorates obesity and liver steatosis by regulating gut microbiota composition in mice. *Food Funct.* **2021**, *12*, 7897–7908. [[CrossRef](#)]
46. Zhang, X.; Coker, O.O.; Chu, E.S.; Fu, K.; Lau, H.C.H.; Wang, Y.-X.; Chan, A.W.H.; Wei, H.; Yang, X.; Sung, J.J.Y.; et al. Dietary cholesterol drives fatty liver-associated liver cancer by modulating gut microbiota and metabolites. *Gut* **2020**, *70*, 761–774. [[CrossRef](#)] [[PubMed](#)]
47. Hu, Y.; Xu, J.; Sheng, Y.; Liu, J.; Li, H.; Guo, M.; Xu, W.; Luo, Y.; Huang, K.; He, X. *Pleurotus ostreatus* Ameliorates Obesity by Modulating the Gut Microbiota in Obese Mice Induced by High-Fat Diet. *Nutrients* **2022**, *14*, 1868. [[CrossRef](#)]
48. Cheng, X.; Jiang, J.; Li, C.; Xue, C.; Kong, B.; Chang, Y.; Tang, Q. The compound enzymatic hydrolysate of *Neoporphyra haitanensis* improved hyperglycemia and regulated the gut microbiome in high-fat diet-fed mice. *Food Funct.* **2022**, *13*, 6777–6791. [[CrossRef](#)]
49. Benson, A.K.; Kelly, S.A.; Legge, R.; Ma, F.; Low, S.J.; Kim, J.; Zhang, M.; Oh, P.L.; Nehrenberg, D.; Hua, K.; et al. Individuality in gut microbiota composition is a complex polygenic trait shaped by multiple environmental and host genetic factors. *Proc. Natl. Acad. Sci. USA* **2010**, *107*, 18933–18938. [[CrossRef](#)]
50. Fatima, S.S.; Jamil, Z.; Alam, F.; Malik, H.Z.; Madhani, S.I.; Ahmad, M.S.; Shabbir, T.; Rehmani, M.N.; Rabbani, A. Polymorphism of the renalase gene in gestational diabetes mellitus. *Endocrine* **2016**, *55*, 124–129. [[CrossRef](#)]